Reduction of pseudocritical temperatures of chiral restoration and deconfinement phase transitions in a magnetized PNJL model

Shijun Mao*

School of Science, Xi'an Jiaotong University, Xi'an, Shaanxi 710049, China

(Received 4 May 2024; accepted 10 August 2024; published 3 September 2024)

We investigate the chiral restoration and deconfinement phase transitions under an external magnetic field in the frame of a Pauli-Villars regularized Polyakov loop extended Nambu-Jona-Lasinio model. A running Polyakov loop scale parameter $T_0(eB)$ is introduced to mimic the reaction of the gluon sector to the presence of magnetic fields. It is found that a decreasing $T_0(eB)$ with magnetic fields can realize the inverse magnetic catalysis phenomena of chiral condensates of u and d quarks, increase of Polyakov loop, and the reduction of pseudocritical temperatures of chiral restoration and deconfinement phase transitions.

DOI: 10.1103/PhysRevD.110.054002

I. INTRODUCTION

The study on quantum chromodynamics (QCD) phase structure has been recently extended to include external electromagnetic fields, motivated by the strong magnetic field in the core of compact stars and in the initial stage of relativistic heavy ion collisions [1–42]. Chiral restoration and deconfinement are the two most important QCD phase transitions at finite temperature and magnetic field.

From recent lattice QCD (LQCD) simulations with a physical pion mass [7–13], the chiral condensates of light quarks (u and d) are enhanced by magnetic fields in vacuum, which is the magnetic catalysis phenomena, but they are suppressed by magnetic fields in a high temperature region, which is the inverse magnetic catalysis phenomena. However, the chiral condensates of s quark and u, d quarks with heavy current masses show magnetic catalysis phenomena in the whole temperature region [13,14]. The pseudocritical temperatures of the chiral restoration phase transition of u, d, s quarks drop down with increasing magnetic field. Meanwhile, lattice simulations report that the renormalized Polyakov loop increases with magnetic fields and the transition temperature of deconfinement decreases as the magnetic field grows [7–11].

On the analytical side, in the presence of a uniform external magnetic field $\mathbf{B} = B\mathbf{e}_z$, the energy dispersion of quarks takes the form $E = \sqrt{p_z^2 + 2|QB|l + m^2}$ with the momentum p_z along the direction of the magnetic field and the Landau level $l = 0, 1, 2, \ldots$ [43]. Owing to this fermion dimension reduction, almost all model calculations at mean field level present the magnetic catalysis effect of chiral condensates in the whole temperature region and the increasing pseudocritical temperatures for chiral restoration and deconfinement phase transitions under the external magnetic field; see the review [1–5] and the references therein. How to explain the inverse magnetic catalysis phenomena and the reduction of pseudocritical temperatures for chiral restoration and deconfinement phase transitions is an open question. Many scenarios are proposed [9,15–42], such as magnetic inhibition of mesons, sphalerons, gluon screening effect, weakening of strong coupling, and anomalous magnetic moment.

In this paper, we will revisit the magnetic field effect on chiral restoration and deconfinement phase transitions in terms of the two-flavor and three-flavor Nambu-Jona-Lasinio model with Polyakov loop (PNJL). According to the lattice QCD analysis [9], the interaction between the Polyakov loop and sea quarks may be important for the mechanism of inverse magnetic catalysis and the reduction of transition temperatures. We consider a magnetic field dependent Polyakov loop scale parameter $T_0(eB)$ to mimic the reaction of the gluon sector to the presence of magnetic fields. This type of procedure on parameter T_0 had already been proposed in a different context, such as in the two-flavor Polyakov loop extended quark-meson model (PQM) [38], and three-flavor (entangled) PNJL model [35]. The PQM model [38] reported that the reduction of pseudocritical temperature of chiral restoration happens only in a weak magnetic field region. The PNJL model with a magnetic field independent regularization scheme cannot reproduce the decreasing pseudocritical temperatures for chiral restoration and deconfinement, but the entangled PNJL model can realize it [35]. With a covariant Pauli-Villars regularization scheme in our two-flavor and three-flavor PNJL model, we find that it is possible to account for

*Contact author: maoshijun@mail.xjtu.edu.cn

the inverse magnetic catalysis phenomena of chiral condensates of u, d quarks, increase of Polyakov loop, and the reduction of pseudocritical temperatures of chiral restoration and deconfinement phase transitions, when introducing a fast decreasing $T_0(eB)$.

The paper is organized as follows. Section II is devoted to the two-flavor PNJL model, which introduces the framework in Sec. II A and discusses the numerical results in Sec. II B. A similar study is extended to the three-flavor PNJL model in Sec. III. Finally, we give the summary in Sec. IV.

II. TWO-FLAVOR PNJL MODEL

A. Theoretical framework

The two-flavor PNJL model in external electromagnetic fields is defined through the Lagrangian density [44–52],

$$\mathcal{L} = \bar{\psi}(i\gamma_\mu D^\mu - \hat{m}_0)\psi + \frac{G}{2}\left[(\bar{\psi}\psi)^2 + (\bar{\psi}i\gamma_5\tau\psi)^2\right] - \mathcal{U}(\Phi,\bar{\Phi}). \quad (1)$$

The covariant derivative $D^\mu = \partial^\mu + iQA^\mu - i\mathcal{A}^\mu$ couples quarks to the two external fields, the magnetic field $\mathbf{B} = \nabla \times \mathbf{A}$, and the temporal gluon field $\mathcal{A}^\mu = \delta_0^\mu \mathcal{A}^0$ with $\mathcal{A}^0 = g\mathcal{A}_a^0\lambda_a/2 = -i\mathcal{A}_4$ in Euclidean space. The gauge coupling g is combined with the SU(3) gauge field $\mathcal{A}_a^0(x)$ to define $\mathcal{A}^\mu(x)$, and λ_a are the Gell-Mann matrices in color space. In this work, we consider the magnetic field $\mathbf{B} = (0,0,B)$ along the z axis by setting $A_\mu = (0,0,xB,0)$ in Landau gauge, which couples with quarks of electric charge $Q = \mathrm{diag}(Q_u, Q_d) = \mathrm{diag}(2e/3, -e/3)$. $\hat{m}_0 = \mathrm{diag}(m_0^u, m_0^d) = \mathrm{diag}(m_0, m_0)$ is the current quark mass matrix in flavor space, which controls the explicit breaking of chiral symmetry. For the chiral section in the Lagrangian, G is the coupling constant in the scalar and pseudoscalar channels, which determines the spontaneous breaking of chiral symmetry. The Polyakov potential describing deconfinement at finite temperature reads as

$$\frac{\mathcal{U}(\Phi,\bar{\Phi})}{T^4} = -\frac{b_2(t)}{2}\bar{\Phi}\Phi - \frac{b_3}{6}(\bar{\Phi}^3 + \Phi^3) + \frac{b_4}{4}(\bar{\Phi}\Phi)^2, \quad (2)$$

where Φ is the trace of the Polyakov loop $\Phi = (\mathrm{Tr}_c L)/N_c$, with $L(\mathbf{x}) = \mathcal{P}\exp[i\int_0^\beta d\tau A_4(\mathbf{x},\tau)] = \exp[i\beta A_4]$ and $\beta = 1/T$, the coefficient $b_2(t) = a_0 + a_1 t + a_2 t^2 + a_3 t^3$ with $t = T_0/T$ is temperature dependent, and the other coefficients b_3 and b_4 are constants.

The order parameter to describe chiral restoration phase transition is the chiral condensate $\sigma = \langle\bar{\psi}\psi\rangle$ or the dynamical quark mass $m = m_0 - G\sigma$ [53–57]. Φ is considered as the order parameter to describe the deconfinement phase transition, which satisfies $\Phi \to 0$ in confined phase at low temperature and $\Phi \to 1$ in deconfined phase at high temperature [44–52]. In mean field approximation, the thermodynamic potential at finite temperature and magnetic field contains the mean field part and quark part,

$$\Omega_{\mathrm{mf}} = \mathcal{U}(\Phi,\bar{\Phi}) + \frac{(m-m_0)^2}{2G} + \Omega_q,$$
$$\Omega_q = -\sum_{f,n}\alpha_n \int \frac{dp_z}{2\pi}\frac{|Q_f B|}{2\pi}\Big[3E_f + T\ln\left(1 + 3\Phi e^{-\beta E_f} + 3\bar{\Phi}e^{-2\beta E_f} + e^{-3\beta E_f}\right) + T\ln\left(1 + 3\bar{\Phi}e^{-\beta E_f} + 3\Phi e^{-2\beta E_f} + e^{-3\beta E_f}\right)\Big], \quad (3)$$

with spin factor $\alpha_n = 2 - \delta_{n0}$ and quark energy $E_f = \sqrt{p_z^2 + 2n|Q_f B| + m^2}$ of flavor $f = u$, d and Landau level n.

The ground state is determined by minimizing the thermodynamic potential,

$$\frac{\partial\Omega_{\mathrm{mf}}}{\partial m} = 0, \qquad \frac{\partial\Omega_{\mathrm{mf}}}{\partial\Phi} = 0, \qquad \frac{\partial\Omega_{\mathrm{mf}}}{\partial\bar{\Phi}} = 0, \quad (4)$$

which leads to three coupled gap equations for the order parameters m, Φ, and $\bar{\Phi}$. Note that there is $\Phi = \bar{\Phi}$ at vanishing baryon density. Therefore, in our current work, we only need to solve two coupled gap equations,

$$\frac{\partial\Omega_{\mathrm{mf}}}{\partial m} = 0, \qquad \frac{\partial\Omega_{\mathrm{mf}}}{\partial\Phi} = 0. \quad (5)$$

Because of the contact interaction among quarks, Nambu-Jona-Lasinio (NJL) models are nonrenormalizable, and it is necessary to introduce a regularization scheme to remove the ultraviolet divergence in momentum integrations. In this work, we take a Pauli-Villars regularization [16], which is gauge invariant and can guarantee the law of causality at finite magnetic field. The three parameters in the two-flavor NJL model, namely the current quark mass $m_0 = 5$ MeV, the coupling constant $G = 7.79\ \mathrm{GeV}^{-2}$, and the mass parameter $\Lambda = 1127$ MeV are fixed by fitting the chiral condensate $\langle\bar{\psi}\psi\rangle = (-250\ \mathrm{MeV})^3$, pion mass $m_\pi = 134$ MeV, and pion decay constant $f_\pi = 93$ MeV in vacuum. For the Polyakov potential, the parameters are chosen as [45] $a_0 = 6.75$, $a_1 = -1.95$, $a_2 = 2.625$, $a_3 = -7.44$, $b_3 = 0.75$, $b_4 = 7.5$, and we consider two cases $T_0 = 270$ MeV and $T_0 = 210$ MeV in the following numerical calculations.

B. Numerical results

As we know, the model parameter $T_0 = 270$ MeV is the critical temperature for the deconfinement phase transition in the pure gauge Polyakov loop model, and the inclusion of dynamical quarks will lead to a decrease of T_0 [51,52]. The external magnetic field makes the change on the quark properties, so that it will also alter the value of parameter T_0. This modification in the Polyakov potential will

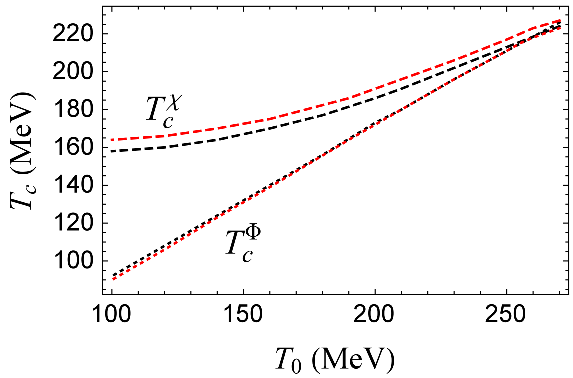

FIG. 1. The pseudocritical temperatures T_c^χ, T_c^Φ of chiral restoration and deconfinement phase transitions as functions of parameter T_0 with fixed magnetic field $eB/m_\pi^2 = 0$ (black lines) and $eB/m_\pi^2 = 10$ (red lines).

affect the chiral restoration and deconfinement phase transitions under external magnetic fields. In this work, we introduce a magnetic field dependent parameter $T_0(eB)$ to mimic the reaction of gluon sector to the presence of magnetic fields, and consider its effect on the chiral restoration and deconfinement phase transitions.

In Fig. 1, we plot the pseudocritical temperatures T_c^χ, T_c^Φ for chiral restoration and deconfinement phase transitions as functions of parameter T_0 with fixed magnetic field $eB/m_\pi^2 = 0$ (black lines) and $eB/m_\pi^2 = 10$ (red lines). At finite temperature and/or magnetic field, the chiral restoration and deconfinement phase transitions are smooth crossover. The pseudocritical temperature T_c^χ is defined by the condition $\frac{\partial^2 m}{\partial T^2} = 0$, and T_c^Φ is defined by $\frac{\partial^2 \Phi}{\partial T^2} = 0$. On one side, with fixed magnetic fields, the pseudocritical temperatures T_c^χ and T_c^Φ decrease as T_0 decreases. Moreover, T_c^Φ decreases faster than T_c^χ, which results in a larger separation between them at a smaller value of T_0. The reason is the direct influence of the Polyakov loop parameter T_0 on the gluon sector and indirect influence on the quark sector. On the other side, when fixing T_0, T_c^χ is higher with stronger magnetic fields, which is the typical result of mean field calculations in effective models [1–5]. T_c^Φ is not sensitive to the magnetic field, because there is no direct interaction between the magnetic field and gluon field. Considering the effects of parameter T_0 and external magnetic field eB on chiral restoration and deconfinement phase transitions, we can expect that with a fast decreasing T_0 under magnetic fields, it is possible to observe the reduction of pseudocritical temperatures T_c^χ and T_c^Φ as the magnetic field grows.

1. $T_0(eB=0)=270$ MeV

The upper panel of Fig. 2 shows two explicit examples of magnetic field dependent $T_0(eB)$ with $T_0(eB = 0) = 270$ MeV. In the case of $T_0^{(1)}(eB)$ (see the blue line in the upper panel), we obtain a constant pseudocritical temperature of chiral restoration T_c^χ with different magnetic fields.

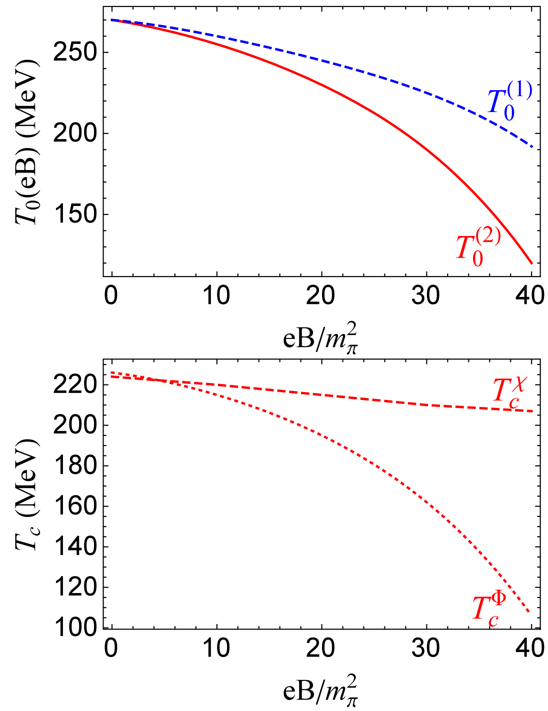

FIG. 2. Upper panel: two examples of magnetic field dependent parameter T_0 in the Polyakov potential, $T_0^{(1)}(eB)$ (blue line) and $T_0^{(2)}(eB)$ (red line), with $T_0(eB = 0) = 270$ MeV. Lower panel: the pseudocritical temperatures T_c^χ, T_c^Φ for chiral restoration and deconfinement phase transitions as functions of magnetic fields with $T_0^{(2)}(eB)$.

It should be mentioned that due to separation between T_c^χ and T_c^Φ, it is not possible to obtain constant T_c^χ and T_c^Φ simultaneously. When we have a faster decreasing $T_0^{(2)}(eB)$ (see the red line in the upper panel), both pseudocritical temperatures T_c^χ, T_c^Φ of chiral restoration and deconfinement phase transitions (see the lower panel) decrease with increasing magnetic fields, which show a similar trend as LQCD results [7–13]. However, T_c^χ and T_c^Φ have different decreasing slope when the magnetic field grows. The pseudocritical temperature of chiral restoration T_c^χ is influenced by the magnetic field and parameter T_0. T_c^χ becomes larger with a stronger magnetic field, but becomes smaller with a smaller value of T_0. Their competition leads to a slow decreasing slope for T_c^χ. T_c^Φ is not sensitive to the magnetic field but decreases as T_0 decreases. Therefore, we observe a larger splitting between T_c^χ and T_c^Φ at stronger magnetic field, which is different from LQCD results [7–13].

When we obtain the reduction of pseudocritical temperatures T_c^χ, T_c^Φ of chiral restoration and deconfinement phase transitions, such as in the case of $T_0^{(2)}(eB)$, what is the behavior of the order parameters at finite temperature and/or magnetic field? In Fig. 3, the chiral condensate σ/σ_0 (upper panel) and Polyakov loop Φ (lower panel) are

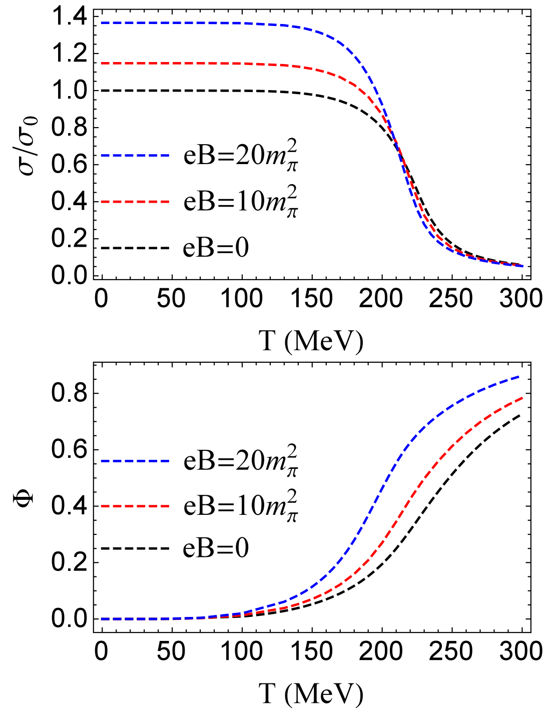

FIG. 3. The order parameters, chiral condensate σ/σ_0 (upper panel), and Polyakov loop Φ (lower panel) as functions of temperature with fixed magnetic field $eB/m_\pi^2 = 0$, 10, 20 and $T_0^{(2)}(eB)$. Here, σ_0 is the chiral condensate in vacuum with vanishing temperature, density, and magnetic field.

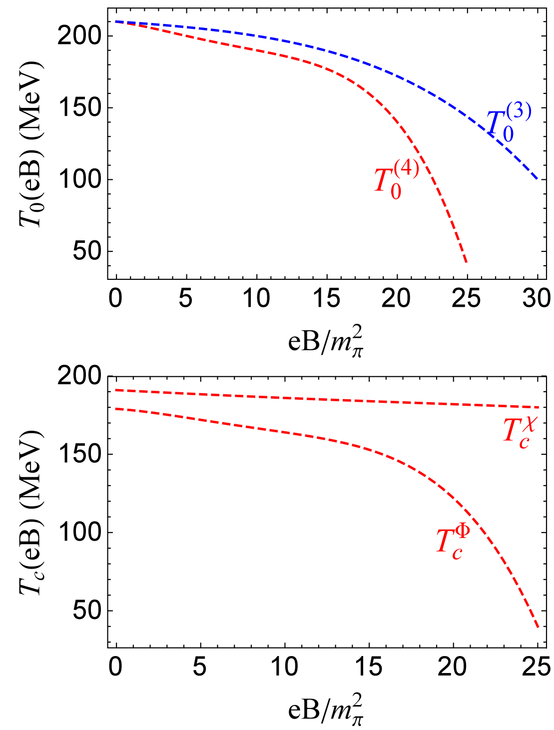

FIG. 4. Upper panel: two examples of magnetic field dependent parameter T_0 in Polyakov potential, $T_0^{(3)}(eB)$ (blue line) and $T_0^{(4)}(eB)$ (red line), with $T_0(eB = 0) = 210$ MeV. Lower panel: the pseudocritical temperatures T_c^χ, T_c^Φ for chiral restoration and deconfinement phase transitions as functions of magnetic fields with $T_0^{(4)}(eB)$.

depicted as functions of temperature with fixed magnetic field $eB/m_\pi^2 = 0$, 10, 20 and $T_0^{(2)}(eB)$. Here, σ_0 is the chiral condensate in vacuum with vanishing temperature, density, and magnetic field. With a fixed magnetic field, the chiral condensate σ/σ_0 decreases with temperature, which indicates the restoration of chiral symmetry, and the Polyakov loop Φ increases with temperature, which means the occurrence of deconfinement. At the low temperature region, the chiral condensate σ/σ_0 increases with magnetic fields, which shows magnetic catalysis phenomena, but at the high temperature region, the chiral condensate σ/σ_0 decreases with magnetic fields, which shows inverse magnetic catalysis phenomena. The Polyakov loop Φ increases with magnetic fields in the whole temperature region. These properties are consistent with LQCD simulations [7–13].

2. $T_0(eB = 0) = 210$ MeV

The inclusion of dynamical quarks leads to a decrease of T_0 at vanishing magnetic field, and in the two-flavor PNJL model, $T_0(eB = 0) = 210$ MeV is also widely used.

The upper panel of Fig. 4 shows two explicit examples of magnetic field dependent $T_0(eB)$ with $T_0(eB = 0) = 210$ MeV. In the case of $T_0^{(3)}(eB)$ (see the blue line in the upper panel), we obtain a constant pseudocritical temperature of chiral restoration T_c^χ with different magnetic fields. $T_0^{(3)}(eB)$ approaches less than $T_0^{(3)}(eB=0)/2$ at $eB=30m_\pi^2$. Comparing with $T_0^{(1)}(eB)$ in Fig. 2, $T_0^{(3)}(eB)$ decreases faster than $T_0^{(1)}(eB)$, as the magnetic field increases.

When introducing a faster decreasing $T_0(eB)$, such as $T_0^{(4)}(eB)$ in the upper panel of Fig. 4, we obtain a decreasing critical temperature T_c^χ, T_c^Φ for chiral restoration and deconfinement phase transitions under the external magnetic field (see Fig. 4, lower panel). Comparing with the results of $T_0(eB = 0) = 270$ MeV in Fig. 2, the reduction of T_c^χ and T_c^Φ in the case of $T_0(eB = 0) = 210$ MeV happens in a narrower window of magnetic fields, and there still appears splitting between T_c^χ and T_c^Φ. Moreover, in the case of $T_0^{(4)}(eB)$, we calculate the order parameters at finite temperature and/or magnetic field. The results look similar as in Fig. 3, and we do not show/discuss it in this part.

III. THREE-FLAVOR PNJL MODEL

A. Theoretical framework

The three-flavor PNJL model under external magnetic field is defined through the Lagrangian density [44–50],

$$\mathcal{L} = \bar{\psi}(i\gamma^\mu D_\mu - \hat{m}_0)\psi + \mathcal{L}_S + \mathcal{L}_6 - \mathcal{U}(\Phi,\bar{\Phi}),$$
$$\mathcal{L}_S = G\sum_{\alpha=0}^{8}[(\bar{\psi}\lambda_\alpha\psi)^2 + (\bar{\psi}i\gamma_5\lambda_\alpha\psi)^2],$$
$$\mathcal{L}_6 = -K[\det\bar{\psi}(1+\gamma_5)\psi + \det\bar{\psi}(1-\gamma_5)\psi],$$
$$\mathcal{U}(\Phi,\bar{\Phi}) = T^4\left[-\frac{b_2(t)}{2}\bar{\Phi}\Phi - \frac{b_3}{6}(\bar{\Phi}^3+\Phi^3) + \frac{b_4}{4}(\bar{\Phi}\Phi)^2\right]. \tag{6}$$

The covariant derivative $D^\mu = \partial^\mu + iQA^\mu - i\mathcal{A}^\mu$ couples quarks to the two external fields, the magnetic field $\mathbf{B} = \nabla\times\mathbf{A}$, and the temporal gluon field $\mathcal{A}^\mu = \delta_0^\mu\mathcal{A}^0$ with $\mathcal{A}^0 = g\mathcal{A}_a^0\lambda_a/2 = -i\mathcal{A}_4$ in Euclidean space. The gauge coupling g is combined with the SU(3) gauge field $\mathcal{A}_a^0(x)$ to define $\mathcal{A}^\mu(x)$, and λ_a are the Gell-Mann matrices in color space. We consider the magnetic field $\mathbf{B} = (0,0,B)$ along the z axis by setting $A_\mu = (0,0,xB,0)$ in Landau gauge, which couples quarks of electric charge $Q = \mathrm{diag}(Q_u,Q_d,Q_s) = \mathrm{diag}(2/3e,-1/3e,-1/3e)$. $\hat{m}_0 = \mathrm{diag}(m_0^u,m_0^d,m_0^s)$ is the current quark mass matrix in flavor space. The four-fermion interaction $\mathcal{L}_S$ represents the interaction in scalar and pseudoscalar channels, with Gell-Mann matrices $\lambda_\alpha, \alpha = 1,2,\ldots,8$ and $\lambda_0 = \sqrt{2/3}\mathbf{I}$ in flavor space. The six-fermion interaction or Kobayashi-Maskawa-'t Hooft term $\mathcal{L}_6$ is related to the $U_A(1)$ anomaly [58–61]. The Polyakov potential $\mathcal{U}(\Phi,\bar{\Phi})$ describes deconfinement at finite temperature, where Φ is the trace of the Polyakov loop $\Phi = (\mathrm{Tr}_c L)/N_c$, with $L(\mathbf{x}) = \mathcal{P}\exp[i\int_0^\beta d\tau A_4(\mathbf{x},\tau)] = \exp[i\beta A_4]$ and $\beta = 1/T$, the coefficient $b_2(t) = a_0 + a_1t + a_2t^2 + a_3t^3$ with $t = T_0/T$ is temperature dependent, and the other coefficients b_3 and b_4 are constants.

It is useful to convert the six-fermion interaction into an effective four-fermion interaction in the mean field approximation, and the Lagrangian density can be rewritten as [62]

$$\begin{aligned}\mathcal{L} = {}& \bar{\psi}(i\gamma^\mu D_\mu - \hat{m}_0)\psi - \mathcal{U}(\Phi,\bar{\Phi}) + \sum_{a=0}^{8}\left[K_a^-(\bar{\psi}\lambda^a\psi)^2 + K_a^+(\bar{\psi}i\gamma_5\lambda^a\psi)^2\right] + K_{30}^-(\bar{\psi}\lambda^3\psi)(\bar{\psi}\lambda^0\psi) + K_{30}^+(\bar{\psi}i\gamma_5\lambda^3\psi)(\bar{\psi}i\gamma_5\lambda^0\psi)\\ &+ K_{03}^-(\bar{\psi}\lambda^0\psi)(\bar{\psi}\lambda^3\psi) + K_{03}^+(\bar{\psi}i\gamma_5\lambda^0\psi)(\bar{\psi}i\gamma_5\lambda^3\psi) + K_{80}^-(\bar{\psi}\lambda^8\psi)(\bar{\psi}\lambda^0\psi) + K_{80}^+(\bar{\psi}i\gamma_5\lambda^8\psi)(\bar{\psi}i\gamma_5\lambda^0\psi)\\ &+ K_{08}^-(\bar{\psi}\lambda^0\psi)(\bar{\psi}\lambda^8\psi) + K_{08}^+(\bar{\psi}i\gamma_5\lambda^0\psi)(\bar{\psi}i\gamma_5\lambda^8\psi) + K_{83}^-(\bar{\psi}\lambda^8\psi)(\bar{\psi}\lambda^3\psi) + K_{83}^+(\bar{\psi}i\gamma_5\lambda^8\psi)(\bar{\psi}i\gamma_5\lambda^3\psi)\\ &+ K_{38}^-(\bar{\psi}\lambda^3\psi)(\bar{\psi}\lambda^8\psi) + K_{38}^+(\bar{\psi}i\gamma_5\lambda^3\psi)(\bar{\psi}i\gamma_5\lambda^8\psi),\end{aligned} \tag{7}$$

with the effective coupling constants

$$\begin{aligned}K_0^\pm &= G \pm \frac{1}{3}K(\sigma_u+\sigma_d+\sigma_s),\\ K_1^\pm &= K_2^\pm = K_3^\pm = G \mp \frac{1}{2}K\sigma_s,\\ K_4^\pm &= K_5^\pm = G \mp \frac{1}{2}K\sigma_d,\\ K_6^\pm &= K_7^\pm = G \mp \frac{1}{2}K\sigma_u,\\ K_8^\pm &= G \mp \frac{1}{6}K(2\sigma_u+2\sigma_d-\sigma_s),\\ K_{03}^\pm &= K_{30}^\pm = \mp\frac{1}{2\sqrt{6}}K(\sigma_u-\sigma_d),\\ K_{08}^\pm &= K_{80}^\pm = \mp\frac{\sqrt{2}}{12}K(\sigma_u+\sigma_d-2\sigma_s),\\ K_{38}^\pm &= K_{83}^\pm = \pm\frac{1}{2\sqrt{3}}K(\sigma_u-\sigma_d),\end{aligned} \tag{8}$$

and chiral condensates

$$\sigma_u = \langle\bar{u}u\rangle, \qquad \sigma_d = \langle\bar{d}d\rangle, \qquad \sigma_s = \langle\bar{s}s\rangle. \tag{9}$$

The thermodynamic potential in the mean field level contains the mean field part and quark part,

$$\begin{aligned}\Omega_{\mathrm{mf}} &= 2G(\sigma_u^2+\sigma_d^2+\sigma_s^2) - 4K\sigma_u\sigma_d\sigma_s + \mathcal{U}(\Phi,\bar{\Phi}) + \Omega_q,\\ \Omega_q &= -\sum_{f=u,d,s}\frac{|Q_fB|}{2\pi}\sum_l\alpha_l\int\frac{dp_z}{2\pi}\big[3E_f\\ &\quad + T\ln\left(1+3\Phi e^{-\beta E_f}+3\bar{\Phi}e^{-2\beta E_f}+e^{-3\beta E_f}\right)\\ &\quad + T\ln\left(1+3\bar{\Phi}e^{-\beta E_f}+3\Phi e^{-2\beta E_f}+e^{-3\beta E_f}\right)\big],\end{aligned}$$

with quark energy $E_f = \sqrt{p_z^2+2l|Q_fB|+m_f^2}$ of flavor $f = u,\ d,\ s$, longitudinal momentum p_z, Landau level l, and effective quark masses $m_u = m_0^u - 4G\sigma_u + 2K\sigma_d\sigma_s$, $m_d = m_0^d - 4G\sigma_d + 2K\sigma_u\sigma_s$, $m_s = m_0^s - 4G\sigma_s + 2K\sigma_u\sigma_d$, and the degeneracy of Landau levels $\alpha_l = 2 - \delta_{l0}$. The ground state is determined by minimizing the thermodynamic potential,

$$\frac{\partial\Omega_{\rm mf}}{\partial\sigma_i} = 0, \qquad i = u, d, s,$$
$$\frac{\partial\Omega_{\rm mf}}{\partial\Phi} = 0, \qquad \frac{\partial\Omega_{\rm mf}}{\partial\bar{\Phi}} = 0, \tag{10}$$

which leads to five coupled gap equations for the order parameters σ_i, Φ, and $\bar{\Phi}$. Note that there is $\Phi = \bar{\Phi}$ at vanishing baryon density.

Because of the contact interaction in the NJL model, the ultraviolet divergence cannot be eliminated through renormalization, and a proper regularization scheme is needed. In this part, we also apply the covariant Pauli-Villars regularization [16]. By fitting the physical quantities, pion mass $m_\pi = 138$ MeV, pion decay constant $f_\pi = 93$ MeV, kaon mass $m_K = 495.7$ MeV, and η' meson mass $m_{\eta'} = 957.5$ MeV in vacuum, we fix the current masses of light quarks $m_0^u = m_0^d = 5.5$ MeV, and obtain the parameters $m_0^s = 154.7$ MeV, $G\Lambda^2 = 3.627$, $K\Lambda^5 = 92.835$, $\Lambda = 1101$ MeV [63]. For the Polyakov potential, the parameters are chosen as [45] $a_0 = 6.75$, $a_1 = -1.95$, $a_2 = 2.625$, $a_3 = -7.44$, $b_3 = 0.75$, $b_4 = 7.5$, and we consider two cases $T_0 = 270$ MeV and $T_0 = 190$ MeV in the following numerical calculations.

B. Numerical results

1. $T_0(eB=0)=270$ MeV

As in the two-flavor PNJL model, we introduce a running Polyakov loop parameter $T_0(eB)$ in the three-flavor PNJL model, and consider its effect on the chiral restoration and deconfinement phase transitions. With $T_0(eB=0) = 270$ MeV, our numerical results for $T_0(eB)$, which solves a constant critical temperature for chiral restoration in u/d quarks, are very close to $T_0^{(1)}(eB)$ in Fig. 2. In the following numerical calculations, we also use $T_0(eB) = T_0^{(2)}(eB)$ (shown in the red line of Fig. 2, upper panel) as an example.

The pseudocritical temperatures of chiral restoration and deconfinement phase transitions under external magnetic field with running parameter $T_0(eB) = T_0^{(2)}(eB)$ are listed in Table I. In the nonchiral limit, the chiral restoration and deconfinement phase transitions at finite temperature and magnetic field are smooth crossover. The pseudocritical temperature of chiral restoration $T_c^f(f = u, d, s)$ is usually defined through the vanishing second derivative of the chiral condensate, $\frac{\partial^2\sigma_f}{\partial T^2} = 0$. The pseudocritical temperature of deconfinement T_c^Φ is defined by the vanishing second derivative of the Polyakov loop, $\frac{\partial^2\Phi}{\partial T^2} = 0$. All the pseudocritical temperatures $T_c^{u,d,s}$ and T_c^Φ decrease with magnetic fields, which is qualitatively consistent with LQCD results [7–13]. Owing to different electric charges of u and d quarks, the corresponding pseudocritical temperatures T_c^u and T_c^d under external magnetic field are slightly deviated from each other ($T_c^d \leq T_c^u$). The pseudocritical temperature T_c^s is larger than T_c^u and T_c^d ($T_c^d \leq T_c^u < T_c^s$), which is caused by its heavier current quark mass. The pseudocritical temperature T_c^Φ of the deconfinement phase transition is close to the T_c^u and T_c^d in weak magnetic field cases, but becomes split with T_c^u and T_c^d in strong magnetic field cases, which is not consistent with LQCD results [7–13].

Figure 5 shows the chiral condensates $\sigma_u/\sigma_{u0}, \sigma_d/\sigma_{d0}, \sigma_s/\sigma_{s0}$ and Polyakov loop Φ as functions of temperature with fixed magnetic field $eB/m_\pi^2 = 0$, 10, 20 and $T_0^{(2)}(eB)$. Here, $\sigma_{u0}, \sigma_{d0}, \sigma_{s0}$ means up, down, strange quark chiral condensate in vacuum with vanishing temperature, density, and magnetic field, respectively. With fixed magnetic field, the chiral condensates $\sigma_u/\sigma_{u0}, \sigma_d/\sigma_{d0}, \sigma_s/\sigma_{s0}$ decrease with temperature, which demonstrates the (partial) restoration of chiral symmetry, and the Polyakov loop Φ increases with temperature, which indicates the deconfinement process. With fixed temperature, the chiral condensates $\sigma_u/\sigma_{u0}, \sigma_d/\sigma_{d0}, \sigma_s/\sigma_{s0}$ increase with magnetic fields in the low temperature region, which is the magnetic catalysis phenomena, but in the high temperature region, they decrease with magnetic fields, which is the inverse magnetic catalysis phenomena. Polyakov loop Φ increases with magnetic fields in the whole temperature region. The results of u and d quark condensates and Polyakov loop Φ are consistent with LQCD results [7–13], but the LQCD results of the magnetic catalysis effect for the s quark condensate in the whole temperature region [13,14] cannot be reproduced here.

TABLE I. Results of pseudocritical temperatures for chiral restoration and deconfinement phase transitions under external magnetic field with running parameter $T_0(eB) = T_0^{(2)}(eB)$.

eB (m_π^2)	$T_0(eB)$ (MeV)	T_c^u (MeV)	T_c^d (MeV)	T_c^s (MeV)	T_c^Φ (MeV)
0	270	215	215	268	216
10	255	212	211	261	207
20	230	209	208	253	192
30	190	205	203	241	160

2. $T_0(eB=0)=190$ MeV

The inclusion of dynamical quarks leads to a decrease of T_0 at vanishing magnetic field, and in the three-flavor PNJL model, $T_0(eB=0) = 190$ MeV is usually used. As indicated in Fig. 6, with a lower value of $T_0(eB=0)$, a fast decreasing $T_0(eB)$, such as $T_0^{(6)}$ can realize the decreasing of critical temperatures of chiral restoration and deconfinement phase transitions. Comparing with the case with $T_0(eB=0) = 270$ MeV in Table I, the reduction of T_c^f and T_c^Φ in the case of $T_0(eB=0) = 190$ MeV happens in a narrower window of magnetic fields, and splitting still

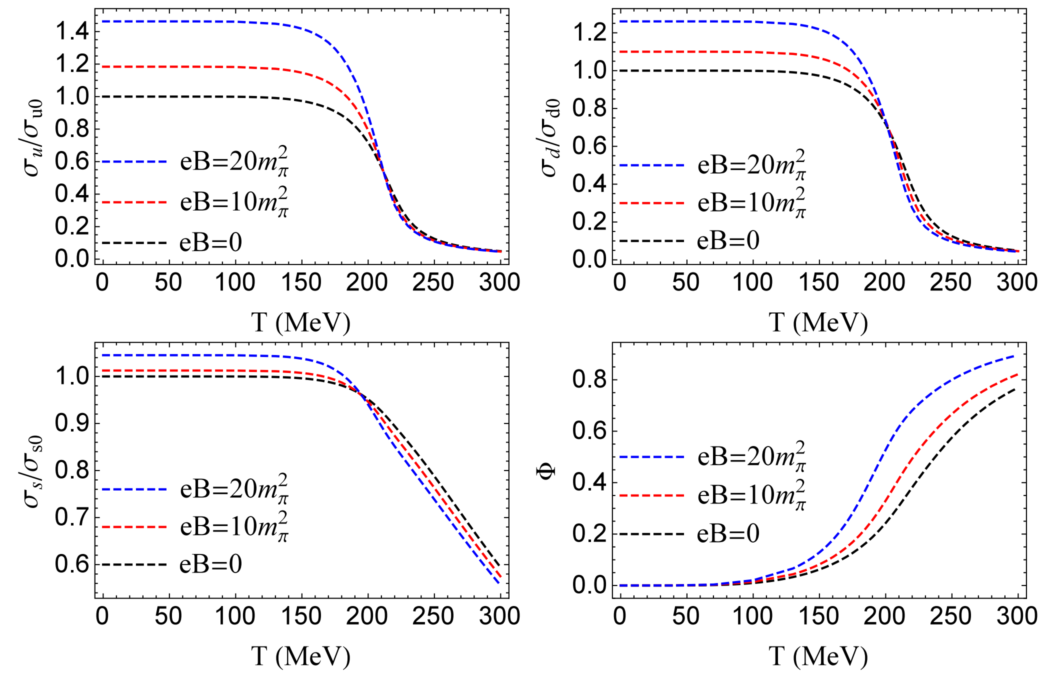

FIG. 5. The chiral condensates $\sigma_u/\sigma_{u0}, \sigma_d/\sigma_{d0}, \sigma_s/\sigma_{s0}$, and Polyakov loop Φ as functions of temperature with fixed magnetic field $eB/m_\pi^2 = 0$, 10, 20 and $T_0^{(2)}(eB)$. Here, $\sigma_{u0}, \sigma_{d0}, \sigma_{s0}$ means up, down, strange quark chiral condensate in vacuum with vanishing temperature, density, and magnetic field, respectively.

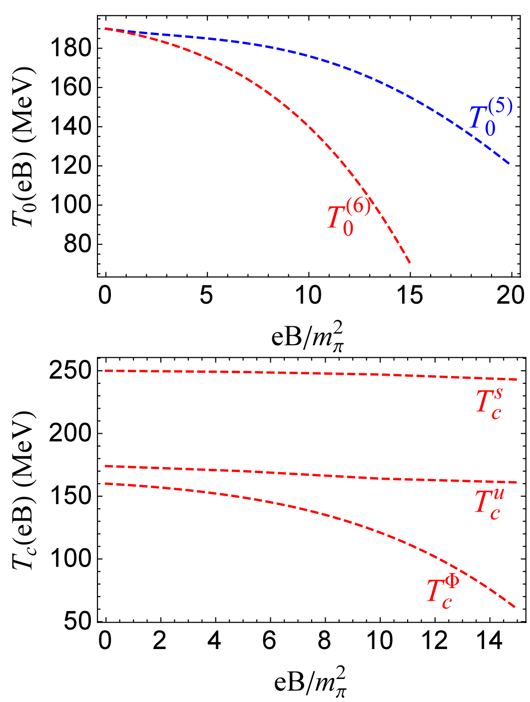

FIG. 6. Upper panel: two examples of magnetic field dependent parameter T_0 in Polyakov potential, $T_0^{(5)}(eB)$ (blue line) and $T_0^{(6)}(eB)$ (red line), with $T_0(eB = 0) = 190$ MeV. Lower panel: the pseudocritical temperatures T_c^u, T_c^s, T_c^Φ for chiral restoration and deconfinement phase transitions as functions of magnetic fields with $T_0^{(6)}(eB)$.

appears between T_c^f and T_c^Φ. Moreover, in the case of $T_0^{(6)}(eB)$, we calculate the order parameters at finite temperature and/or magnetic field. The results look similar as in Fig. 5, and we therefore do not show/discuss it in this part.

IV. SUMMARY

We investigate the chiral restoration and deconfinement phase transitions under external magnetic field in terms of Pauli-Villars regularized two-flavor and three-flavor PNJL models. To mimic the reaction of the gluon sector to the presence of magnetic fields, we introduce the running Polyakov loop scale parameter $T_0(eB)$. It was found that a fast decreasing $T_0(eB)$ with the magnetic field leads to the inverse magnetic catalysis phenomena of chiral condensates of u, d, s quarks, increase of the Polyakov loop, and the reduction of pseudocritical temperatures of chiral restoration and deconfinement phase transitions. Our conclusions are qualitatively independent of the choice of logarithmic or polynomial form of Polyakov potential and the value of parameter $T_0(eB = 0)$ at vanishing magnetic field.

Our results of the two-flavor PNJL model are consistent with those in the two-flavor PQM model [38]. But the results of the three-flavor PNJL model are opposite to Ref. [35], which concluded that $T_0(eB)$ cannot reproduce the decreasing pseudocritical temperatures for chiral restoration and deconfinement phase transitions. The difference is attributed to the different regularization schemes. In Ref. [35], a magnetic field independent regularization scheme is applied, which introduced a three-momentum noncovariant cutoff to regularize the divergent momentum integrals in vacuum (vanishing temperature, density, and magnetic field). In our work, we apply the covariant Pauli-Villars regularization in vacuum (vanishing temperature, density, and magnetic field) and in medium (finite temperature, density, and magnetic field).

All these results are qualitatively consistent with LQCD simulations, except for the chiral condensate of s quarks, and the splitting between the pseudocritical temperatures of chiral restoration and deconfinement phase transitions. To solve the discrepancy, other physical factors should also be introduced, such as the magnetic field dependent quark coupling constant [25,26], and the entanglement between the quarks and the Polyakov loop [35,64,65], which will be considered in our future work.

ACKNOWLEDGMENTS

The work is supported by the NSFC Grant No. 12275204.

[1] F. Preis, A. Rebhan, and A. Schmitt, Lect. Notes Phys. **871**, 51 (2013).
[2] R. Gatto and M. Ruggieri, Lect. Notes Phys. **871**, 87 (2013).
[3] V. A. Miransky and I. A. Shovkovy, Phys. Rep. **576**, 1 (2015).
[4] J. O. Anderson and W. R. Naylor, Rev. Mod. Phys. **88**, 025001 (2016).
[5] G. Q. Cao, Eur. Phys. J. A **57**, 264 (2021).
[6] M. D'Elia, Lect. Notes Phys. **871**, 181 (2013).
[7] G. S. Bali, F. Bruckmann, G. Endrodi, Z. Fodor, S. D. Katz, S. Krieg, A. Schaefer, and K. K. Szabo, J. High Energy Phys. 02 (2012) 044.
[8] G. S. Bali, F. Bruckmann, G. Endrodi, Z. Fodor, S. D. Katz, and A. Schaefer, Phys. Rev. D **86**, 071502 (2012); J. High Energy Phys. 08 (2014) 177.
[9] F. Bruckmann, G. Endrodi, and T. G. Kovacs, J. High Energy Phys. 04 (2013) 112.
[10] V. G. Bornyakov, P. V. Buividovich, N. Cundy, O. A. Kochetkov, and A. Schaefer, Phys. Rev. D **90**, 034501 (2014).
[11] G. Endrodi, J. High Energy Phys. 07 (2015) 173.
[12] G. Endrodi, M. Giordano, S. D. Katz, T. G. Kovacs, and F. Pittler, J. High Energy Phys. 07 (2019) 009.
[13] H. T. Ding, S. T. Li, J. H. Liu, and X. D. Wang, Phys. Rev. D **105**, 034514 (2022).
[14] M. D'Elia, F. Manigrasso, F. Negro, and F. Sanfilippo, Phys. Rev. D **98**, 054509 (2018).
[15] K. Fukushima and Y. Hidaka, Phys. Rev. Lett. **110**, 031601 (2013).
[16] S. J. Mao, Phys. Lett. B **758**, 195 (2016); Phys. Rev. D **94**, 036007 (2016); **97**, 011501(R) (2018); Chin. Phys. C **45**, 021004 (2021); Phys. Rev. D **106**, 034018 (2022).
[17] K. Kamikado and T. Kanazawa, J. High Energy Phys. 03 (2014) 009.
[18] J. Y. Chao, P. C. Chu, and M. Huang, Phys. Rev. D **88**, 054009 (2013).
[19] J. Braun, W. A. Mian, and S. Rechenberger, Phys. Lett. B **755**, 265 (2016).
[20] N. Mueller and J. M. Pawlowski, Phys. Rev. D **91**, 116010 (2015).
[21] T. Kojo and N. Su, Phys. Lett. B **720**, 192 (2013).
[22] A. Ayala, M. Loewe, A. J. Mizher, and R. Zamora, Phys. Rev. D **90**, 036001 (2014).
[23] A. Ayala, L. A. Hernandez, A. J. Mizher, J. C. Rojas, and C. Villavicencio, Phys. Rev. D **89**, 116017 (2014).
[24] A. Ayala, C. A. Dominguez, L. A. Hernandez, M. Loewe, and R. Zamora, Phys. Rev. D **92**, 096011 (2015).
[25] R. L. S. Farias, K. P. Gomes, G. Krein, and M. B. Pinto, Phys. Rev. C **90**, 025203 (2014).
[26] M. Ferreira, P. Costa, O. Lourenco, T. Frederico, and C. Providência, Phys. Rev. D **89**, 116011 (2014).
[27] F. Preis, A. Rebhan, and A. Schmitt, J. High Energy Phys. 03 (2011) 033.
[28] E. S. Fraga and A. J. Mizher, Phys. Rev. D **78**, 025016 (2008); Nucl. Phys. **A820**, 103c (2009).
[29] K. Fukushima, M. Ruggieri, and R. Gatto, Phys. Rev. D **81**, 114031 (2010).
[30] C. V. Johnson and A. Kundu, J. High Energy Phys. 12 (2008) 053.
[31] V. Skokov, Phys. Rev. D **85**, 034026 (2012).
[32] E. S. Fraga, J. Noronha, and L. F. Palhares, Phys. Rev. D **87**, 114014 (2013).
[33] R. Gatto and M. Ruggieri, Phys. Rev. D **82**, 054027 (2010); **83**, 034016 (2011).
[34] M. Ferreira, P. Costa, and C. Providência, Phys. Rev. D **89**, 036006 (2014).
[35] M. Ferreira, P. Costa, D. P. Menezes, and C. Providência, and N. N. Scoccola, Phys. Rev. D **89**, 016002 (2014).
[36] P. Costa, M. Ferreira, H. Hansen, D. P. Menezes, and C. Providência, Phys. Rev. D **89**, 056013 (2014).
[37] A. J. Mizher, M. N. Chernodub, and E. S. Fraga, Phys. Rev. D **82**, 105016 (2010).
[38] E. S. Fraga, B. W. Mintz, and J. Schaffner-Bielich, Phys. Lett B **731**, 154 (2014).
[39] E. J. Ferrer, V. de la Incera, I. Portillo, and M. Quiroz, Phys. Rev. D **89**, 085034 (2014).
[40] E. J. Ferrer, V. de la Incera, and X. J. Wen, Phys. Rev. D **91**, 054006 (2015).
[41] J. Mei and S. J. Mao, Phys. Rev. D **102**, 114035 (2020).
[42] K. Xu, J. Y. Chao, and M. Huang, Phys. Rev. D **103**, 076015 (2021).
[43] L. D. Landau and E. M. Lifshitz, *Quantum Mechanics* (Elservier Butterworth-Heinemann, London, 1938).
[44] P. N. Meisinger and M. C. Ogilvie, Phys. Lett. B **379**, 163 (1996).

[45] P. N. Meisinger, T. R. Miller, and M. C. Ogilvie, Phys. Rev. D **65**, 034009 (2002).
[46] K. Fukushima, Phys. Lett. B **591**, 277 (2004).
[47] A. Mocsy, F. Sannino, and K. Tuominen, Phys. Rev. Lett. **92**, 182302 (2004).
[48] E. Megias, E. Ruiz Arriola, and L. L. Salcedo, Phys. Rev. D **74**, 065005 (2006).
[49] C. Ratti, M. A. Thaler, and W. Weise, Phys. Rev. D **73**, 014019 (2006); arXiv:nucl-th/0604025.
[50] S. K. Ghosh, T. K. Mukherjee, M. G. Mustafa, and R. Ray, Phys. Rev. D **73**, 114007 (2006).
[51] B. Schaefer, J. M. Pawlowski, and J. Wambach, Phys. Rev. D **75**, 074023 (2007).
[52] S. Roessner, T. Hell, C. Ratti, and W. Seise, Nucl. Phys. **A814**, 118 (2008).
[53] Y. Nambu and G. Jona-Lasinio, Phys. Rev. **122**, 345 (1961); **124**, 246 (1961).
[54] S. P. Klevansky, Rev. Mod. Phys. **64**, 649 (1992).
[55] M. K. Volkov, Phys. Part. Nucl. **24**, 35 (1993).
[56] T. Hatsuda and T. Kunihiro, Phys. Rep. **247**, 221 (1994).
[57] M. Buballa, Phys. Rep. **407**, 205 (2005).
[58] T. Kunihiro and T. Hatsuda, Phys. Lett. B **206**, 385 (1988).
[59] V. Bernard, R. L. Jaffe, and U. G. Meissner, Nucl. Phys. **B308**, 753 (1988).
[60] H. Reinhardt and R. Alkofer, Phys. Lett. B **207**, 482 (1988).
[61] G.'t-Hooft, Phys. Rev. D **14**, 3432 (1976); Phys. Rep. **142**, 357 (1986).
[62] P. Rehberg, S. P. Klevansky, and J. Hüfner, Phys. Rev. C **53**, 410 (1996).
[63] J. Mei, T. Xia, and S. J. Mao, Phys. Rev. D **107**, 074018 (2023).
[64] Y. Sakai, T. Sasaki, H. Kouno, and M. Yahiro, Phys. Rev. D **82**, 076003 (2010).
[65] T. Sasaki, Y. Sakai, H. Kouno, and M. Yahiro, Phys. Rev. D **84**, 091901(R) (2011).